ARTICLE

OPEN ACCESS

Frontiers in earth observation for global soil properties assessment linked to environmental and socio-economic factors

José A.M. Demattê,[1,2,*] Raul R. Poppiel,[1,2] Jean Jesus Macedo Novais,[1] Nícolas Augusto Rosin,[1] Budiman Minasny,[3] Igor Y. Savin,[4,5] Sabine Grunwald,[6] Songchao Chen,[7,8] Yongsheng Hong,[9] Jingyi Huang,[10] Sabine Chabrillat,[11,12] Quirijn de Jong van Lier,[13] Eyal Ben-Dor,[14] Cecile Gomez,[15,16] Zhang Ganlin,[17] Merilyn Taynara Accorsi Amorim,[1] Letícia Guadagnin Vogel,[1] Jorge Tadeu Fim Rosas,[1] Robert Milewski,[11] Asa Gholizadeh,[18] Arseniy V. Zhogolev,[4] José Padarian Campusano,[3] Yuxin Ma,[3,19] Ho Jun Jang,[3] Rudiyanto,[20] Changkun Wang,[9] Rodnei Rizzo,[13] Nikolaos Tziolas,[6] Nikolaos Tsakiridis,[21] Masakazu Kodaira,[22] D. Nagesh Kumar,[23] Subramanian Dharumarajan,[24] Yufeng Ge,[25] Emmanuelle Vaudour,[26] Shamsollah Ayoubi,[27] James Kobina Mensah Biney,[28] Abdelaziz Belal,[29] Salman Naimi Marandi,[27] Najmeh Asgari Hafshejani,[27] Eleni Kalopesa,[21] Danilo Cesar Mello,[1] Marcio Rocha Francelino,[30] Elsayed Said Mohamed Salama,[5,29] and Asmaa Abdelbaki[11,31]

*Correspondence: jamdemat@usp.br

Received: November 13, 2024; Accepted: June 5, 2025; https://doi.org/10.1016/j.xinn.2025.100985

GRAPHICAL ABSTRACT

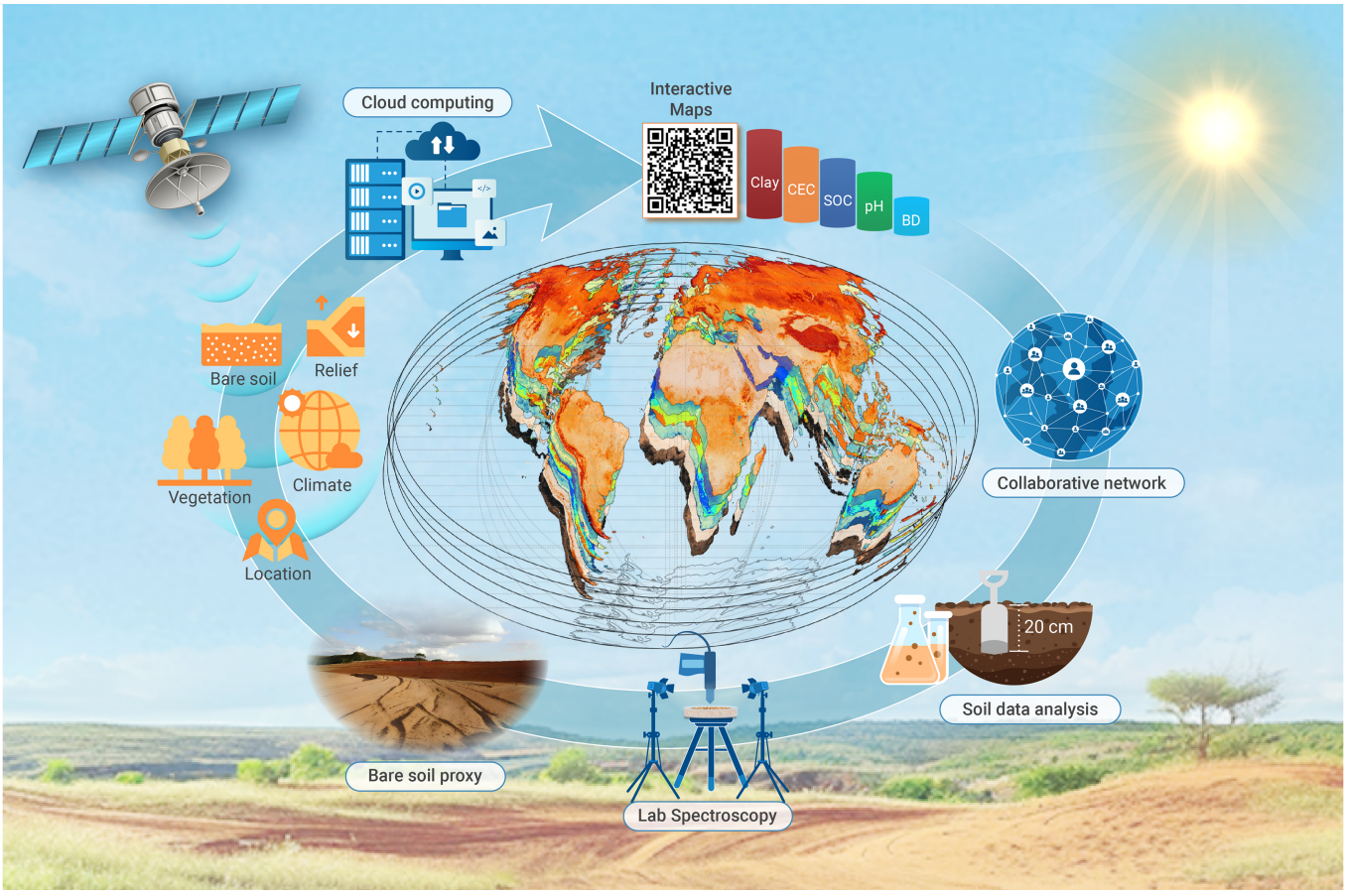

PUBLIC SUMMARY

- Powerful soil-vegetation satellite proxies generated 90-m soil-property maps.
- 64% of the world's topsoil is sandy and highly degradable.
- Global topsoil stores 900 Gt of carbon, of which 54% is in natural vegetation.
- Tillage positively affects fertility by making nutrients available.
- Tillage negatively affects soil health by depleting carbon.
- The top 10 largest countries collectively store 75% of the global carbon stock.

OPEN ACCESS

ARTICLE

The Innovation

Frontiers in earth observation for global soil properties assessment linked to environmental and socio-economic factors

José A.M. Demattê,[1,2,*] Raul R. Poppiel,[1,2] Jean Jesus Macedo Novais,[1] Nícolas Augusto Rosin,[1] Budiman Minasny,[3] Igor Y. Savin,[4,5] Sabine Grunwald,[6] Songchao Chen,[7,8] Yongsheng Hong,[9] Jingyi Huang,[10] Sabine Chabrillat,[11,12] Quirijn de Jong van Lier,[13] Eyal Ben-Dor,[14] Cecile Gomez,[15,16] Zhang Ganlin,[17] Merilyn Taynara Accorsi Amorim,[1] Letícia Guadagnin Vogel,[1] Jorge Tadeu Fim Rosas,[1] Robert Milewski,[11] Asa Gholizadeh,[18] Arseniy V. Zhogolev,[4] José Padarian Campusano,[3] Yuxin Ma,[3,19] Ho Jun Jang,[3] Rudiyanto,[20] Changkun Wang,[9] Rodnei Rizzo,[13] Nikolaos Tziolas,[6] Nikolaos Tsakiridis,[21] Masakazu Kodaira,[22] D. Nagesh Kumar,[23] Subramanian Dharumarajan,[24] Yufeng Ge,[25] Emmanuelle Vaudour,[26] Shamsollah Ayoubi,[27] James Kobina Mensah Biney,[28] Abdelaziz Belal,[29] Salman Naimi Marandi,[27] Najmeh Asgari Hafshejani,[27] Eleni Kalopesa,[21] Danilo Cesar Mello,[1] Marcio Rocha Francelino,[30] Elsayed Said Mohamed Salama,[5,29] and Asmaa Abdelbaki[11,31]

[1]Department of Soil Science, Luiz de Queiroz College of Agriculture, University of São Paulo, Piracicaba 13418-900, São Paulo, Brazil
[2]Center for Carbon Research in Tropical Agriculture (CCARBON), Luiz de Queiroz College of Agriculture, University of São Paulo, Piracicaba 13418-900, São Paulo, Brazil
[3]Sydney Institute of Agriculture & School of Life and Environmental Sciences, The University of Sydney, Sydney, New South Wales, 2006, Australia
[4]V.V. Dokuchaev Soil Science Institute, Moscow 119017, Russia
[5]Department of Environmental Management, Institute of Environmental Engineering, RUDN University, Moscow, Russia
[6]Department of Soil, Water, and Ecosystem Sciences, University of Florida, Gainesville, 32611, Florida, USA
[7]ZJU-Hangzhou Global Scientific and Technological Innovation Center, Zhejiang University, Hangzhou 311215, China
[8]College of Environmental and Resource Sciences, Zhejiang University, Hangzhou 310058, China
[9]State Key Laboratory of Soil and Sustainable Agriculture, Institute of Soil Science, Chinese Academy of Sciences, Nanjing 211135, China
[10]Department of Soil and Environmental Sciences, University of Wisconsin – Madison, Madison, Wisconsin, 53706-1380, USA
[11]GFZ Helmholtz Centre for Geosciences, Telegrafenberg, 14473 Potsdam, Germany
[12]Leibniz University Hannover, Institute of Earth System Science, Soil science section, 30419 Hannover, Germany
[13]Center of Nuclear Energy in Agriculture (CENA), University of São Paulo, São Paulo 13416-903, Brazil
[14]Department of Geography, Porter School of Environmental and Earth Sciences, Faculty of Exact Science, Tel Aviv University, Tel Aviv 6997801, Israel
[15]LISAH, University Montpellier, IRD, INRAE, Institut Agro, AgroParisTech, 34060 Montpellier, France
[16]Indo-French Cell for Water Sciences, IRD, Indian Institute of Science, Bengaluru 560012, India
[17]Institute of Soil Science, Chinese Academy of Sciences, Nanjing 210008, China
[18]Department of Soil Science and Soil Protection, Faculty of Agrobiology, Food and Natural Resources, Czech University of Life Sciences Prague, 16500 Prague, Czech Republic
[19]NSW Department of Climate Change, Energy, the Environment and Water, Parramatta, NSW 2150, Australia
[20]Program of Crop Science, Faculty of Fisheries and Food Science, Universiti Malaysia Terengganu, Kuala Nerus 21030, Malaysia
[21]Aristotle University of Thessaloniki, 54124 Thessaloniki, Greece
[22]Institute of Agriculture, Tokyo University of Agriculture and Technology, Fuchu, Tokyo 183-8509 (P4-37), Japan
[23]Department of Civil Engineering, Indian Institute of Science Bangalore, Bengaluru 560012, India
[24]ICAR - National Bureau of Soil Survey and Land Use Planning, Regional Centre, Bangalore 560024, India
[25]Department of Biological Systems Engineering, University of Nebraska-Lincoln, Lincoln, Nebraska 68583, USA
[26]Université Paris-Saclay, INRAE, AgroParisTech, UMR EcoSys, 91120 Palaiseau, France
[27]Department of Soil Science, Isfahan University of Technology, Isfahan 84156-83111, Iran
[28]Centre for Earth Observation Science (CEOS), University of Manitoba, Winnipeg R3T 2N2, Manitoba, Canada
[29]National authority for remote sensing and space sciences NARSS, Cairo, Egypt
[30]Department of Soils, Federal University of Viçosa, Avenue Peter Henry Rolfs, Viçosa 36570-900, Brazil
[31]Soils and Water Department, Faculty of Agriculture, Fayoum University, Fayoum 63514, Egypt
*Correspondence: jamdemat@usp.br

Received: November 13, 2024; Accepted: June 5, 2025; https://doi.org/10.1016/j.xinn.2025.100985

Citation: Demattê J.A.M., Poppiel R.R., Novais J.J.M., et al., (2025). Frontiers in earth observation for global soil properties assessment linked to environmental and socio-economic factors. The Innovation **6(9)**, 100985.

Soil has garnered global attention for its role in food security and climate change. Fine-scale soil-mapping techniques are urgently needed to support food, water, and biodiversity services. A global soil dataset integrated into an Earth observation system and supported by cloud computing enabled the development of the first global soil grid of six key properties at a 90-m spatial resolution. Assessing them from environmental and socio-economic perspectives, we demonstrated that 64% of the world's topsoils are primarily sandy, with low fertility and high susceptibility to degradation. These conditions limit crop productivity and highlight potential risks to food security. Results reveal that approximately 900 Gt of soil organic carbon (SOC) is stored up to 20 cm deep. Arid biomes store three times more SOC than mangroves based on total areas. SOC content in agricultural soils is reduced by at least 60% compared to soils under natural vegetation. Most agricultural areas are being fertilized while simultaneously experiencing a depletion of the carbon pool. By integrating soil capacity with economic and social factors, we highlight the critical role of soil in supporting societal prosperity. The top 10 largest countries in area per continent store 75% of the global SOC stock. However, the poorest countries face rapid organic matter degradation. We indicate an interconnection between societal growth and spatially explicit mapping of soil properties. This soil-human nexus establishes a geographically based link between soil health and human development. It underscores the importance of soil management in enhancing agricultural productivity and promotes sustainable-land-use planning.

INTRODUCTION

Environmental, agricultural, and climate-change research has historically focused on above-ground factors,[1] although soil plays a vital role in the functioning and maintenance of global ecosystems. However, it has been marginalized in conservation and protection strategies[2,3] and hotspots of biodiversity studies.[4] Until the early 2000s, soil was largely overlooked. Since then, soil has received attention because of growing environmental concerns, becoming a prominent topic in international agreements. As soil is one of the largest carbon sinks on Earth,[5–7] its management is critical in carbon sequestration.[8] Soil addresses societal needs for food and energy[9]; connects with smart climate initiatives[10]; and influences global water, energy, and biogeochemical cycles.[11] The recognition of the essential nature of the soil has led to an increase in research assessing soil functions, such as water storage and erosion control,[12] carbon storage and sequestration potential,[13–15] surface temperature effects

Table 1. Set of environmental covariates used for spatial predictions of soil properties worldwide

Factor	Predictor name	Resolution (m)	Source	Reference
Soil, parent material, age, and organisms	soil-vegetation image (six Landsat bands)	30[a]	GEOS3	Demattê et al.[29]
Climate	annual temperature	1,000[a]	CHELSA[b]	Karger et al.[39]
	annual precipitation	1,000[a]		
Relief	elevation	90	MERIT[c]	Safanelli et al.[40]
	slope	90		Theobald et al.[41]
	multiscale topographic position Index	90		Yamazaki et al.[42]
Spatial position	Euclidean distance to rivers	90		Behrens et al.[43]

[a]The native resolution was resampled to 90 m.
[b]Database: CHELSA (Climatologies at High Resolution for the Earth's Land Surface Areas, https://chelsa-climate.org/)
[c]Database: MERIT DEM (Multi-Error-Removed Improved-Terrain Digital Elevation Model, http://hydro.iis.u-tokyo.ac.jp/~yamadai/MERIT_DEM/)

on biodiversity,[16] the provision of ecosystem services,[17] and soil health assessment.[18]

Human-accelerated soil degradation underscores the urgent need for comprehensive and global monitoring of soil conditions. Although significant progress has been made in mapping soil properties worldwide,[19,20] further research is necessary to unravel the ecosystem processes influencing soil health and to assess how these processes vary across different regions. A major challenge is the limited availability of ground soil observation data. As a result, the finest resolution in global soil-property maps is currently limited to 250 × 250 m,[20] which may impact prediction uncertainties, reducing the ability to detect short-range spatial variability and hampering the interpretation of soil properties.[21] Furthermore, many global assessments of soil properties focused predominantly on soil organic carbon (SOC)[14,19,22] and were related to the global carbon cycle.[23] However, carbon dynamics in soils are influenced by numerous factors, particularly mineralogy.[24] In addition to SOC, other properties, such as pH, cation exchange capacity (CEC), and clay content, are key ones in soil productivity[25] and health.[18]

In this study, we elaborated global-extent maps of topsoil properties reflecting various soil processes across biological, chemical, and physical dimensions.[2,26] SOC stocks (SOCSs) are a key biological indicator with significant environmental and economic implications, serving as a proxy for crop productivity, climate-change mitigation, and carbon market valuation. Within the chemical group, CEC supports nutrient retention and storage, while soil pH influences its availability. In the physical category, clay content influences mineralogy, microbiology, and water retention, while bulk density (BD) directly impacts soil health and plant growth.

To achieve this, we employed a fine grid resolution, utilizing remote sensing (RS) data and machine-learning (ML) techniques. Specifically, we introduce Earth observation bare-soil and vegetation proxies to address gaps around the globe. These are fundamentally rooted in the well-documented intrinsic physical relationship between spectral reflectance and soil in proximal studies[27] and for RS studies.[18,28–30] Vegetation impacts soil composition, particularly data from natural forests.[31]

We can consider from the current literature some key gaps in digital soil mapping (DSM) at a global scale,[32] which are the need to (1) obtain more soil observation points, filling the gaps in the current datasets and also covariates more strongly correlated with soil properties; (2) obtain finer spatial resolution products; (3) connect soils with ecological and socio-economic domains through integrated analyses that consider multiple critical soil properties across diverse climates, ecoregions, countries, and other topics; and (4) validate the products directly in the field, despite the statistical parameters.

Thus, this work contributes to filling these gaps by mapping six key soil properties (SOC content and SOCS, clay, pH, CEC, and BD) at a fine spatial resolution with an innovative system. We also discuss in depth the relationship between these properties with land use, climate, soil management, soil health, economic factors, and other topics across the globe. In collaboration with expert partners worldwide, we pooled together a novel global database consisting of public and private. We bring to light the comparison and discussion between data from different science domains.[33] Our research provides compelling insights on soil properties with current global socio-economic challenges, in particular the role of soil in addressing existential issues of climate-change mitigation, water and food security, and biodiversity protection.

MATERIALS AND METHODS

Soil data

We selected key indicators relevant to sustaining healthy and functional soils.[29] We leveraged global open soil databases and reached out to multidisciplinary researchers and organizations worldwide to gather over 150,000 georeferenced soil observations from countries around the world (Figure S1, Supplemental Note 1; Tables S1–S3, Supplemental Note 2). However, some had data access restricted due to institutional policies. The data were harmonized, quality checked, and then merged into a unified database for interpolation to a depth interval of 0–20 cm using an equal-area spline to preserve mass.[34] We specifically focused on the soil properties with high data availability for spanning the soil pillars: biological, SOC (g kg^{-1}) and SOCS (Gt); chemical, CEC ($mmol_c$ kg^{-1}), and pH in water (unitless); and physical, clay content, and BD, g cm^{-3}). The BD was estimated using an improved pedotransfer function.[35]

Environmental covariates

We carefully selected a (parsimonious) set of environmental covariates (Table 1) to represent key soil formation factors, adopting the SCORPAN (soil, climate, organisms, relief, parent material, age, and spatial position) model framework.[36] We used Google Earth Engine (GEE)[37] to retrieve these covariates from RS data, where their pixel sizes were resampled to a target size of 90 m to provide comprehensive spatial predictions. The soil-vegetation image represented the factors related to soil, parent material, age, and organisms. It was derived from the Landsat series imagery between 1985 and 2022, processed to retrieve cloud-free surface reflectance of bare surfaces,[38] where remaining gaps due to persistent land cover across time were filled with the reflectance of potential natural (permanent) vegetation using the Geospatial Soil Sensing System (GEOS3).[29] This consists of continuously validating the spectral information acquired by the system, with fieldwork, until reaching the best of its performance. In conclusion, the new GEOS3 passed through 5 years of constant improvement until reaching the final bare-soil image.

Annual mean temperature and precipitation were derived from the CHELSA Bioclimatic dataset[39] to represent climatic influences on soil properties. Topographic factors, including elevation, slope,[40] and multiscale topographic position index,[41] were derived from the MERIT Digital Elevation Model.[42] The factor related to the spatial position was represented by the Euclidean distance from sites to rivers equal to or greater than the third level of Strahler's ordination system.[43]

Soil-property mapping

We processed soil data to match the target spatial resolution by averaging values within a 90 × 90-m area, thus ensuring a single soil-property value per pixel. At each averaged soil data site, covariates were sampled to create a comprehensive dataset for modeling. The approach followed the geospatial mapping pipeline[44] using a fully Python-based workflow implemented on Google Colab. The cloud infrastructure, including Google Cloud Storage and GEE, supports data-storage, processing, and computational needs. This framework enabled streamlined handling of our large geospatial datasets, facilitating the integration and analysis of soil data and environmental covariates for mapping of soil properties worldwide.

Table 2. List of global data crossed with our soil-property maps

Category	Description	References
Climate zones	updated Köppen-Geiger climate zones	Beck et al.[46]
Terrestrial ecoregions	ecoregions focusing on vegetation types within the 14 major world ecoregions	Olson et al.[47]
Countries	196 political subdivisions across the world	N/A
Continents	six densely populated regions of the planet	N/A
World	all mapped Earth area	N/A
Land use and land cover	different land uses and land cover, considering stratification by largest countries by area, continents, climate zones, and biomes	Zanaga et al.[48]
GDP	total and *per capita* mean values from 2021–2028 projections for the 20 wealthiest, intermediate, and poorest countries	International Monetary Fund[49]
Gross product of agriculture	total mean value reported from 2022 to 2022 for 20 countries with higher, intermediate, and lower production values countries	Food and Agriculture Organization of the United Nations[50]
Share of the population in extreme poverty	share of population living in extreme poverty mean value from 2015 to 2024 (living with less than US$2.15 per day)	World Bank[51]

Model building and optimization

The SCORPAN modeling paradigm[36] predicts individual soil properties (SOC, SOCS, clay, CEC, pH, and BD) using stacked environmental variables as inputs. The model training process involved hyperparameter tuning of a random forest (RF) algorithm,[45] focusing on three key parameters: variables per split, defined as ranges from 4 to the total number of covariates stepped by 4, controlling the number of covariates considered at each tree split; minimum leaf population, tested values of 3, 6, and 9, setting the minimum sample size for each tree leaf; and maximum nodes, set at 500, 1,000, and 1,500, determining the maximum complexity of each tree.

A grid search across these parameters yielded 27 model combinations. Each model was evaluated using 10-fold cross-validation, stratified by biome to ensure representative performance across ecological regions. Performance metrics, including the coefficient of determination (R^2), root-mean-square error (RMSE), and ratio of performance to interquartile range (RPIQ), were calculated. Models were ranked based on the highest mean R^2 scores across all folds, and the top-performing model was selected for final predictions.

Spatial prediction

Bootstrap sampling was used to assess prediction uncertainty and generate ensemble soil maps. The site-specific soil data were resampled 100 times, with each iteration ensuring representative sampling across different biomes. For every bootstrap iteration, a new RF model was trained and applied to classify the study area, resulting in a series of predictive maps. These maps were aggregated to calculate the mean prediction; the ensemble mean of all bootstrap predictions, forming the final soil map; and the uncertainty map, calculated by the difference between the 2.5th and 97.5th percentiles across bootstrap predictions, highlighting areas with higher predictive uncertainty.

Data interpretation

To assess the mapped soil properties across multiple global perspectives, we intersected vector polygon data from diverse sources (Table 2) with our soil-property maps. For each polygon, we computed zonal statistics (including mean and sum) of the soil properties for further analysis. This allowed us to analyze spatial variability and distribution of soil properties within defined geographic and socio-environmental frameworks.

Statistics for biome and soil properties

Canonical correspondence analysis (CCA) was used to investigate the relationship between soil attribute maps (clay, organic carbon, pH, CEC, BD, and organic carbon stock) and the biome map. The CCA is an ordination technique that seeks to identify canonical axes that maximize the correlation between environmental variables (soil properties) and the distribution of groups (biomes). The model was tested for statistical significance using permutations (999 permutations), and the proportion of variance explained by the canonical axes was calculated. The analysis provided canonical correlations, explained variance, and provided a *p* value to assess the global significance of the relationship between biome maps and soil-attribute maps.

RESULTS AND DISCUSSION

Key soil properties at the planetary scale and the model's performance assessment

Our global soil properties reveal spatial patterns under different environments (Figure 1) and are relevant indicators for sustaining healthy and functional soils.[52] We achieve moderate to high model fit with R^2 in the validation phase, varying from the lowest (0.36 for clay content) to the highest (0.57 for SOCS). The increasing RPIQ values of 0.42 (SOC) < 0.47 (CEC) < 1.21 (BD) < 1.32 (SOCS) < 1.50 (clay) < 1.86 (pH) suggest that clay and pH were modeled with the highest accuracy (Figures S1 and S2, Supplemental Note 1) for sample density and uncertainty maps.[53] These values are consistent with other large-scale DSM at continental and global scales (Tables S1–S3, Supplemental Note 2).

The performance of prediction models varied between soil properties due to several factors, including sampling density, covariates' importance, and latitudinal pattern (Figure S1, Supplemental Note 1).[54,55] The dilemma of global soil legacy databases has been the geographical imbalance in soil observation density. Most uncertainties occurred in the Northern Hemisphere, particularly in Russian and Canadian territories (Figure S2, Supplemental Note 1), where there were fewer soil observation points. Globally, CEC maps had the greatest uncertainty and pH the lowest. The global mapping approach also observed this trend.[20,56]

An innovation of the present work compared to other global DSM studies is the use of a soil-reflectance proxy. This proxy is of great importance in spatializing soil data because it is a direct measurement of the topsoil reflectance.[57] The Geospatial Soil Sensing System (GEOS3) demonstrated accurate results in tests[29,30] and is supported by proximal sensing.[27] In areas covered by vegetation, the proxy offers an indirect estimation of soil properties.,[57] which DSM allowed to fill gaps due to permanent vegetation cover. We instructed researchers to visit a field in their country and conduct observations, which were then compared to the soil-property data collected by the system at the same location (Figure S4, Supplemental Note 1). This new GEOS3 system indicates the importance of creating a model based on several field inspections and different validation procedures (quantitative and qualitative, plus field experience) until reaching the best performance (Video S1, Supplemental Note 3, https://esalqgeocis.wixsite.com/english/videos-1).

The literature published over the last decades shows different predicted spatial patterns for SOCSs, suggesting large uncertainties in SOC or BD measurements and estimation methods (Table S1, Supplemental Note 2). For example, global studies reported topsoil (0–30 cm) SOCSs of 504[58] and 577 Gt.[23] Interestingly, these published studies found different results even using the same public legacy soil databases.[59] In contrast, we created a large database, complementing publicly available legacy data with private information. The modeling reached a global SOCS of 900.1 Gt (Figures 1A and S3A) up to a depth of 0–20 cm with an R^2 of 0.57. Our estimate is 32% larger than the stock provided by the FAO (Food and Agriculture Organization of the United Nations), which

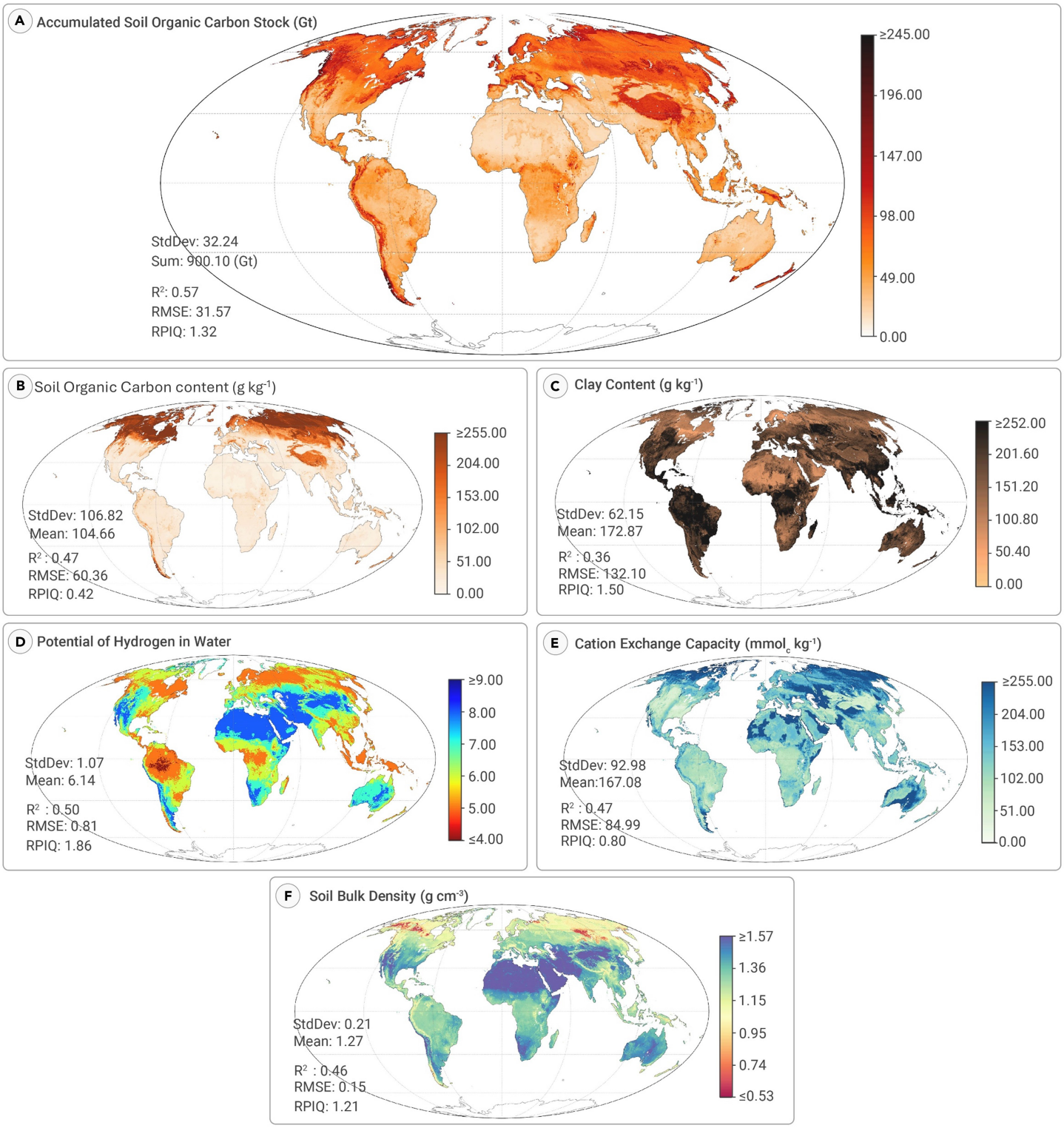

Figure 1. Maps of soil properties at 0- to 20-cm depth and 90-m resolution with modeling metrics (A) Soil organic carbon stock (SOCS) in gigatons (Gt); (B) clay content; (C) soil organic carbon content (SOC, g kg^{-1}); (D) pH in water; (E) cation exchange capacity (CEC), and (F) BD. R^2, coefficient of determination; StdDev, standard deviation; RMSE, root-mean-square error; RPIQ, ratio of performance to interquartile distance. SOCS amount discounted icecap and rocks.

estimated 680 Gt of SOCS in topsoils,[60] and 16% larger than that of Padarian et al. (who estimated 793 Gt for the 0- to 30-cm depth in a grid at a resolution of 500 m).[15] Hiederer and Köchy[58] estimated SOCSs between 710 and 1,459 Gt for the 0- to 100-cm layer, and Scharleman et al.[7] reported a median of 1,437 Gt for the same depth and from 27 individual studies. We reached 900.1 Gt SOCS (0–20 cm), which is within the range estimated by other studies (Table S1, Supplemental Note 2).

We utilized a comprehensive, multi-source dataset spanning the globe, filling important data gaps. Our dataset performed a greater soil observation point density in some regions, such as South America and Asia (Figure S1 , Supplemental Note 1) than for the World Soil Information Service (WoSIS, https://www.isric.org/explore/wosis)[59]. For example, in Asia, we increased from 4,176 to 16,274 from open-access to open-access + private data, respectively. With this upgrade, we observed a greater variation in the SOC amplitude. This improved geographic representation suggests better reliability in the model. Previous studies have not utilized bare-soil proxies or vegetation data within ML frameworks to predict soil properties worldwide, nor have they mapped at a fine spatial resolution. Literature

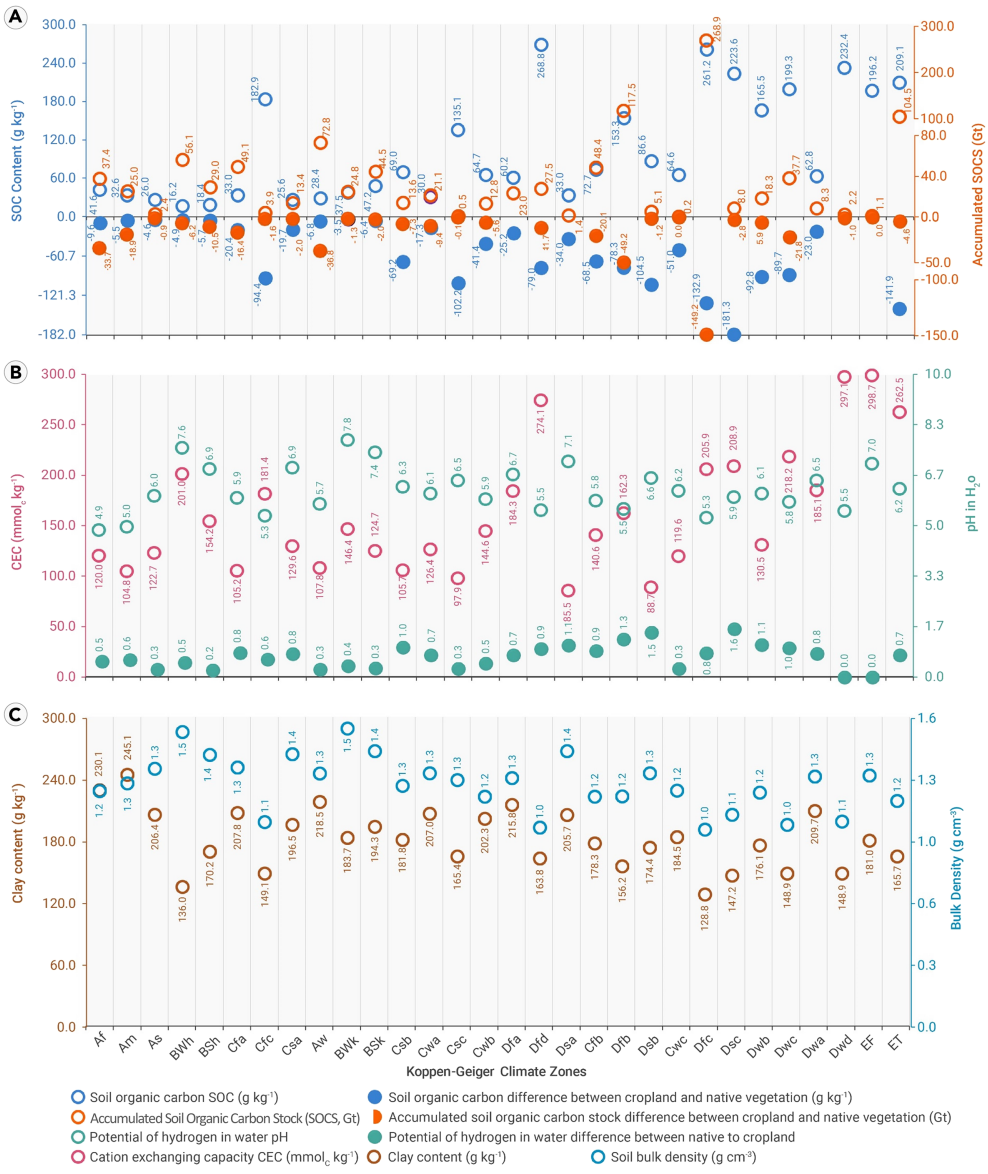

Figure 2. Soil properties in the Köppen-Geiger climate zones[46] (A) Soil organic carbon (SOC) content (blue circles), soil organic carbon stock (SOCS, orange circles); (B) cation exchange capacity (CEC, pink circles) and pH in water (green circles); and (C) clay content (brown circles) and BD (cyan circles). The respective blue, orange, and green spheres represent the SOC, SOCS, and pH differences between the cultivated areas and the native vegetation. Af, tropical rainforest; Am, tropical monsoon; Aw, tropical savanna; BWh, arid desert hot; BWk, arid desert cold; BSh, arid steppe hot; BSk, arid steppe cold; Csa, temperate dry summer hot summer; Csb, temperate dry summer warm summer; Csc, temperate dry summer cold summer; Cwa, temperate dry winter hot summer; Cwb, temperate dry winter warm summer; Cwc, temperate dry winter cold summer; Cfa, temperate no dry season hot summer; Cfb, temperate no dry season warm summer; Cfc, temperate no dry season cold summer; Dsa, cold dry summer hot summer; Dsb, cold dry summer warm summer; Dsc, cold dry summer cold summer; Dsd, cold dry summer very cold winter; Dwa, cold dry winter hot summer; Dwb, cold dry winter warm summer; Dwc, cold dry winter cold summer; Dwd, cold dry winter very cold winter; Dfa, cold no dry season hot summer; Dfb, cold no dry season warm summer; Dfc, cold no dry season cold summer; Dfd, cold no dry season very cold winter; EF, polar frost; ET, polar tundra.

shows that the smaller pixel sizes result in a gain of spatial details, improving the performance of DSM.[61] Despite this, prediction accuracy is inversely correlated with spatial resolution.[62,63] These differences can be seen by visual inspection (Figure S4, Supplemental Note 1).

In an entire area with native vegetation in South America, FAO carbon-content maps indicate abruptly different values. Our map indicated similar values in the area, which is consistent with the same land use observed (native vegetation). The visual inspection is impacted by the improvements of a fine-resolution map, compared with the FAO (1,000 m). A consistency between land uses and SOCS (Figure S4B, Supplemental Note 1) was achieved. We also compared our data with soil grids (Figure S4A, Supplemental Note 1). Visual inspection of our maps revealed that certain regions covering South America, Europe, and Asia exhibited higher SOCS values when compared to the 250-m one. A field profile inspection from China (Figure S4C, Supplemental Note 1) presented a very deep and dark pattern caused by a high carbon horizon at the surface, which agrees with the same spot detected on the map.

We found that more than half of the world's land area (64.5%) consists of sandy soils (soil clay content below 200 g kg^{-1}) (including sand, loamy sand, and sandy loam), while 31.7% of areas have loamy soils and only 3.7% is clayey (clay content over 200 g kg^{-1}). Areas with the highest clay values are in South America, reflecting its geology and greater weathering. Low clay content can be associated with sandy soils, a texture prevalent in desert areas and coastal plains (i.e., southeastern US coastal plains or soils formed in glacial till parent material). These soils typically exhibit low productivity, limiting agricultural production in extensive areas, particularly under technological constraints limitations.[21]

We observed the lowest soil pH values (acidic soils) in equatorial regions such as sub-Saharan Africa, South America, and Indonesia, as well as in some temperate regions of the Northern Hemisphere rich in biomass (Figure 1). Dry-hot regions such as the Sahara presented the highest pH (alkaline soils). While soil pH is largely controlled by parent rock at local and regional scales, it is also modulated by climate and anthropogenic activities. Water balance controls soil pH in dry climates, resulting in basic soils, while, in wet climates, it produces acid.[53] Agricultural management, especially mineral fertilizer applications, has been attributed to a significant decrease in pH values.

A meta-analysis of agricultural soils in China found that, under the long-term application of nitrogen fertilizers in China (1980–2024), soil pH decreased by 15.2%.[64] Soil acidification has been linked to increased losses in inorganic carbon and elevated carbon dioxide (CO_2) emissions, degrading soil health and crop production.[65] Mean pH decreased significantly by 0.3 units with afforestation in a global meta-analysis,[66] suggesting that acidification is amplified through land-use change, which can cause significant depletion of microbial diversity and community composition.[64] Higher BDs were found in desert areas, which have sandy soils rich in quartz. BD is used to calculate SOC stock and nutrient storage[67] and, thus, has major significance in producing accurate global SOCS and SOC sequestration assessments from a local to global scale. Some areas dominated by clayey soils in Brazil presented low BDs, highlighting its relationship with soil compaction and water infiltration capacity reduction.[68]

The CEC is an indicator of nutrient retention, for which we calculated a mean value of 167.1 mmol$_c$ kg^{-1} (Figure 1). The highest nutrient-holding capacities were found in temperate environments, such as South Australia, Europe, East Asia, and North Africa. CEC usually keeps a direct relationship with soil mineralogy and fertility and represents the total capacity of the soil to hold exchangeable cations required by plants.[69]

Benchmarking soil properties by climatic zones

We organized the soil properties distribution in Figure 2 according to the 30 climate zones of Köppen-Geiger.[46] The highest values of SOC (261.2 g kg^{-1}) and SOCS (268.9 Gt) were found in the humid continental zone with a very

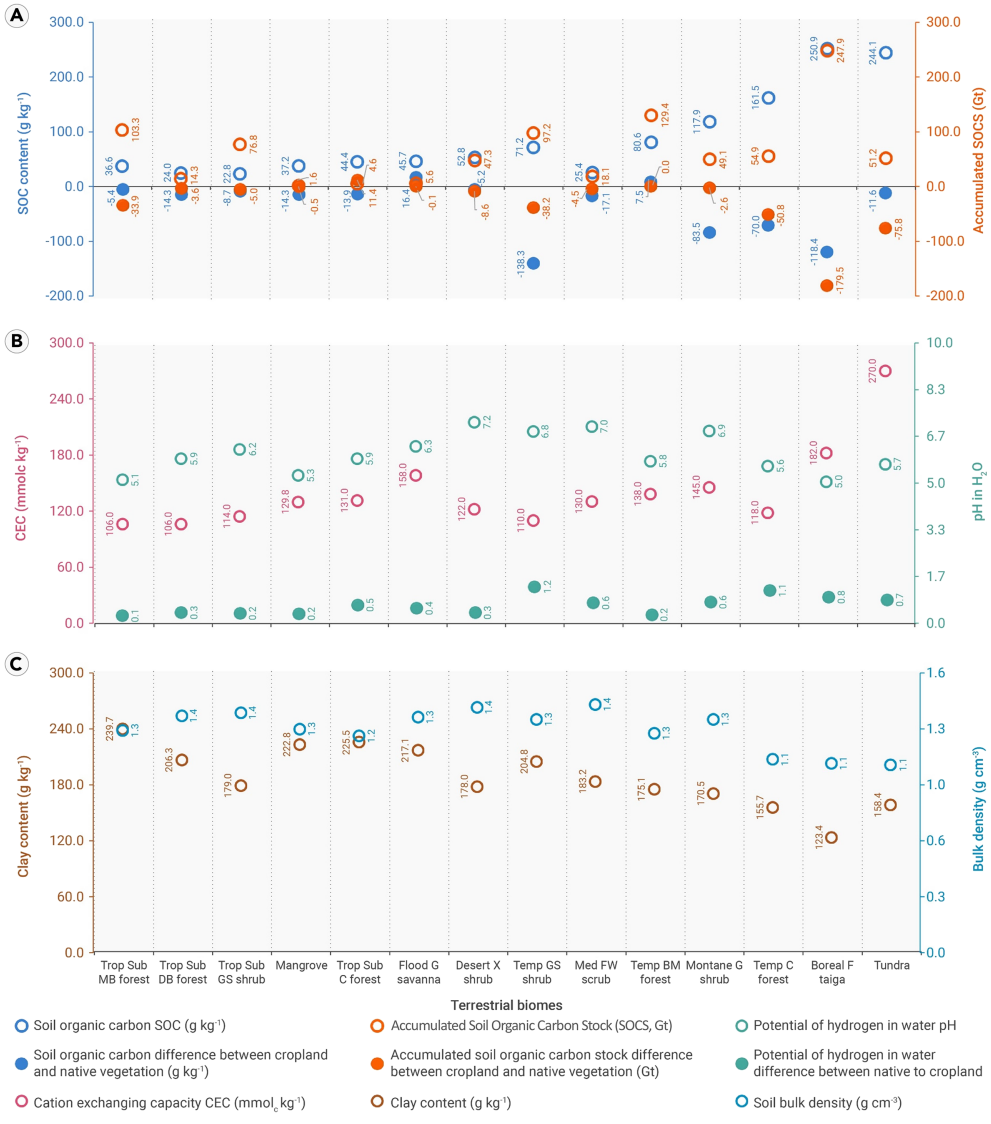

Figure 3. Soil properties in 14 world ecoregions[47]
(A) Soil organic carbon (SOC) content (blue circles) and soil organic carbon stock (SOCS, orange circles), (B) cation exchange capacity (CEC, pink circles) and pH in water (green circles), and (C) clay content (brown circles) and BD (cyan circles). The respective blue, orange, and green spheres represent the SOC, SOCS, and pH differences between the cultivated areas and the native vegetation. Boreal F Taiga, boreal forests/Taiga; Desert X Shrub, deserts and xeric shrublands; Flood G Savanna, flooded grasslands and savannas; Med FW Scrub, Mediterranean forests, woodlands, and scrub; Montane G Shrub, montane grasslands and shrublands; Temp BM Forest, temperate broadleaf and mixed forests; Temp C Forest, temperate conifer forests; Temp GS Shrub, temperate grasslands, savannas, and shrublands; Trop Sub C Forest, tropical and subtropical coniferous forests; Trop Sub DB Forest, tropical and subtropical dry broadleaf forests; Trop Sub GS Shrub, tropical and subtropical grasslands, savannas, and shrublands; Trop Sub MB Forest, tropical and subtropical moist broadleaf forests.

cool summer, in contrast to the lowest values (25.6 g kg^{-1} and 13.4 Gt, respectively) in the warm Mediterranean zone (dry, mild summer). This demonstrates a close relationship between organic matter (OM) and climate, which controls the biomass input and decomposition rates.[70]

The cold deserts with freezing winters had the highest mean CEC values (297.1 $mmol_c$ kg^{-1}). The most acidic soils (pH 4.9) were found in the tropical monsoon climate zone due to geological factors and high-intensity weathering. In contrast, hot deserts with a pronounced dry winter season had a mean pH value of 7.8. The CEC and pH influenced weathering processes through base leaching and acidification.[10] Croplands show higher pH values than native areas, up to 1.6 (Figure 2C). This may result from anthropogenic management practices such as fertilizing, irrigating, and liming. In Israel, there are examples of very sandy soils with high pH detected by the mapping system (Figure S5, Supplemental Note 1). Very high- or low-pH soil conditions can reduce the availability of essential plant nutrients and adversely affect plant growth.[71] The physical characteristics are also driven by climate, and such patterns are observed in our results (Figure 2C). In tropical climates, soils were more clayey and with a higher BD than in temperate climates. This is in agreement with Zhao et al.[72] The higher SOC content (Figure 2A) explains the low BD in temperate regions. Finally, the lower clay contents and higher BD were found in arid climates.

Distribution of soil properties in major ecoregions

The highest SOCS and SOC values were found in the boreal forest/Taiga (247.9 Gt and 250.9 g kg^{-1}, respectively) in temperate climates at the extremes of the Northern Hemisphere (Figure 3A). Deserts, despite having the lowest SOC values due to minimal biomass inputs and high temperatures, contained a significant amount, holding 47.27 Gt. This was four times greater than mangroves, which stored 10.8 Gt but covered a much smaller area. While it is generally acknowledged that cold ecoregions had a high SOCS, followed by tropical rainforests, our findings highlight the importance of desert soils. Despite their seemingly inhospitable nature, desert regions are crucial for soil carbon storage, underscoring the importance of sustainable management practices to preserve and enhance these ecosystems. Nevertheless, the high SOCS values in some areas may be uncertain, primarily due to the modeling from cold deserts, such as in the Gobi Desert in China, which often contain rocks and other features with low SOC content (Figures 1A and 1B).

Soil acidity worldwide shows distinct distribution patterns. Alkaline soils were found in arid environments (Figures 3B and S5, Supplemental Note 1), such as Iran with deserts, xeric shrublands, and Mediterranean forests. Conversely, long-time intense weathering processes in tropical ecoregions led to high chemical dissolution and leaching, resulting in acidic soils. Consistently, clay content was higher in tropical ecoregions and lower in temperate ones, such as boreal forests/Taiga and temperate broadleaf and mixed forests. This ecoregion had lower BD values than other areas due to the high OM content (Figure 3C). The association between the soil-property maps and ecoregions was consistent with the distribution of soil classes worldwide.[73,74]

CCA revealed a significant relationship between soil properties and the world's biomes. The variance explained by this technique reached 55.3%, indicating that more than half of the variability in soil properties is associated with biome distribution. The canonical correlation for the first axis was 0.338, demonstrating a moderate association between biomes and soil properties, showing the influence of biomes on soil.

SOCS, SOC, and pH affected by LULC

We observed the influence of human activities, especially agriculture, on global soil properties by comparing them across different land-use and land-cover scenarios (LULCs). For example, soils under native vegetation in Asia exhibited the highest values of SOC and SOCS (Figures 4A and 4B), attributed to climate. Tropical regions, such as South America and Africa, had lower SOC and SOCS values despite the broad areas of native vegetation. The impact of human activities on OM depletion is well known. Standardizing this LULC per area unit, native vegetation regions stored 96.1 t ha^{-1} SOC while cropland stored 59.1 t ha^{-1}. This implies that 37.0 t ha^{-1} more SOCS were stored in the soil under naturally vegetated areas compared to agricultural land.[75] Our values for SOCS are consistent with the results of a similar study that estimated

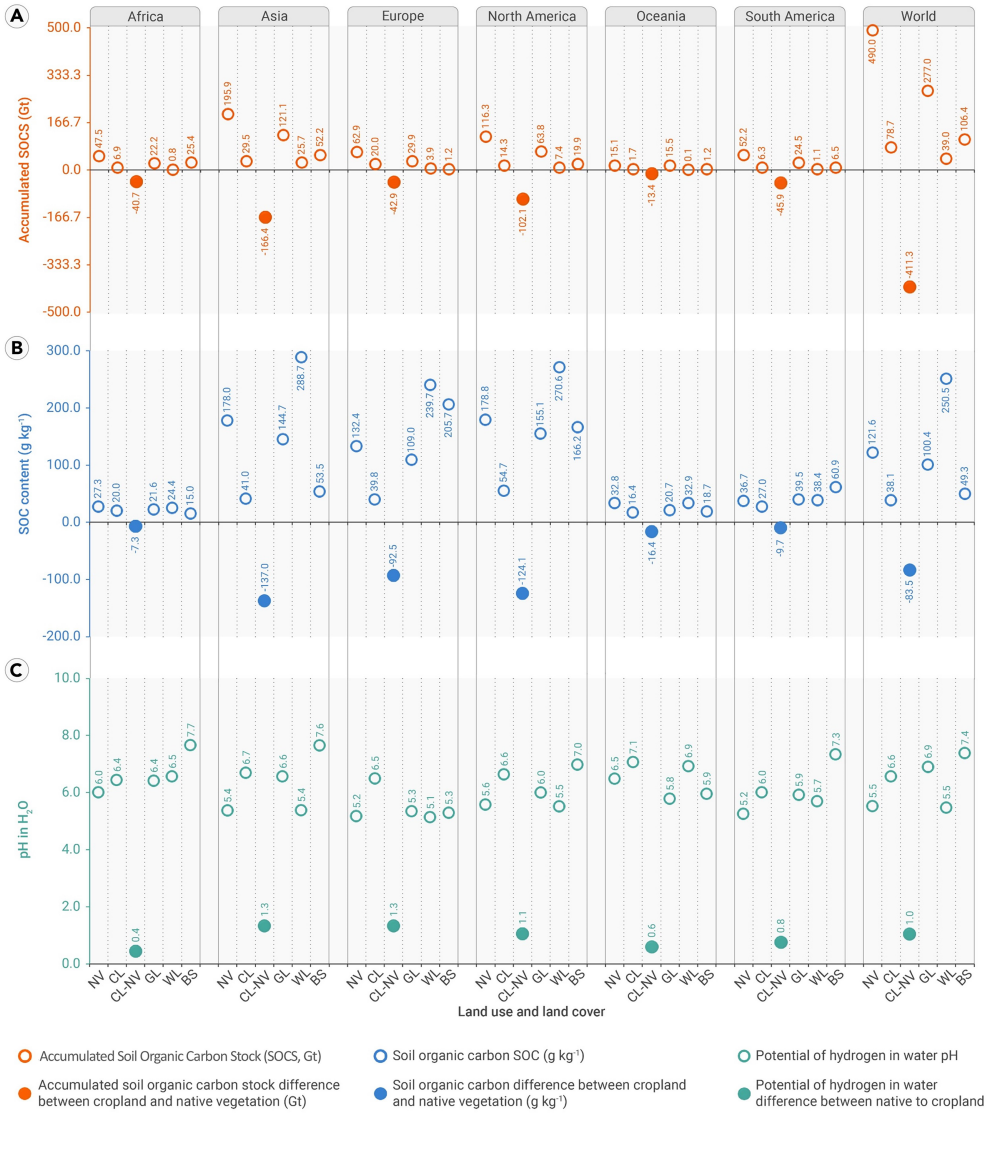

Figure 4. Soil properties chart of land use and land cover[47] in the six continents and the world (A) Soil organic carbon stock (SOCS, orange circles), (B) soil organic carbon content (SOC, blue circles), and (C) pH in water (green circles). The respective orange, blue, and green spheres represent SOCS, SOC, and pH differences between the cultivated areas and the native vegetation. NV, native vegetation; CL, cropland; CL-NV, cropland minus native vegetation; GL, grassland; WL, wetland; BS, bare surface.

that SOC is lost due to land-use change. Native vegetation covered the largest area on the planet (40.73 million km^2) and stored 490 Gt, while cropland stored 79 Gt of SOCS in 15.73 million km^2, a difference of 411 Gt (Figure 4A). Grasslands, which encompassed natural and cultivated pasturelands, accounted for 277.0 Gt of SOCS. We highlight the significant role of natural ecosystems in carbon sequestration despite the rise of anthropogenic activities. In the native vegetation areas, the global average SOC is 121.6 g kg^{-1}, in contrast to only 38.1 g kg^{-1} in croplands (Figure 4B), representing about 60% less SOC. As expected, waterlogged areas showed a significantly higher mean SOC content (250.5 g kg^{-1}) – Figure 4B. These wetland areas are characterized by the accumulation of soil OM due to low levels of aeration, high soil moisture, occasional flooding, and the presence of a water-table fluctuations.[76]

We observed that soils under native vegetation presented lower pH values than croplands in all regions (Figure 4B). Anthropogenic activities affect soil chemistry (pH) on both sides, for good (when fertilizers are applied) and for depletion (when they are not applied). Thus, this higher pH on agricultural lands may be due to soil anthropic management (e.g., liming). Agricultural practices that make soils less acidic include liming by limestone, which increases the pH value to a suitable level.[70] During this process, soil tillage is intense and exposed to degradation such as irradiation, variation of temperature, carbon oxidation, and erosion, which generates negative effects on SOC. On the other hand, most of the areas with continuous bare surfaces are found in desert or arid biomes that were predominated by rocks, low precipitation amounts, and no plowing activities. These biomes are characterized by minimal leaching, maintaining the bases in the soil profile, which explains the high pH (7.4).

The use of conservationist agriculture practices, such as no tillage, increases SOC levels[77] and mitigates soil health. This strategy can protect soils from mechanical and weather impacts and maintain biota and water inside the system. Other practices should be agroforestry, biochar, and biodynamic agriculture. These practices generate long-term economic gains through ecosystem services.[78] Crop diversification further boosts agroecosystem productivity by promoting the "rotation effect."[79] Figure S6 in Supplemental Note 1 shows a global SOCS map analysis across biomes[47] and LULC[48] by a heatmap.

A comprehensive review of 377 studies published between 1985 and 2017 found that cover crops increased cash crop yields by 1.15–7.89 times, likely due to improved soil processes.[80] On the other hand, inappropriate management practices, causing hidden soil hunger, can cause yield losses exceeding 40% in cereal grains.[81] Identifying antagonistic or synergistic soil-property spatialization (as presented in this paper) is key to optimizing management strategies.

Geopolitical distribution of soil properties

We observed the soil properties of the top 10 largest countries in land area per continent (Figure 5). Russia, Canada, the United States, China, Brazil, Australia, Kazakhstan, Mongolia, Argentina, India, the Democratic Republic of Congo, Indonesia, Peru, and Papua New Guinea together account for 800 Gt of SOCS, representing 75% of the total SOCS on the Earth's surface. These values are proportional to the ones of the Global SOC Map,[60] which shows 70% located in these countries (Figure S7, Supplemental Note 1). Russia and Canada had the highest mean SOC values, with more than 220 g kg^{-1}. This reveals that the cold climates prevailing in these countries contribute to the slow degradation of OM, allowing SOC to accumulate in the soil.[46]

Crop management and site-specific environmental conditions mainly determine the geographic variation of CEC and pH. CEC was highest in Greenland (Denmark) with 288.9 mmol$_c$ kg^{-1} and lowest in the Democratic Republic of Congo (Africa) with 89.5 mmol$_c$ kg^{-1} (Figure 5B). This figure also shows pH values to range from a mean of 4.8 in Guyana (South America) to 7.7 in Algeria and Libya (Africa), Saudi Arabia, and Iran (Asia). These results (Figures 5A and 5B) illustrate the differences in some soil properties (SOC, SOCS, and pH) between arable land and native vegetation. This arrangement emphasizes that soils from areas with native vegetation tend to have more carbon-related properties than arable lands, confirmed by visual inspection (Figures S3A and S3B, Supplemental Note 1).

Soils from specific volcanic regions showed the highest clay contents (Figure 5C), such as Cuba (284.6 g kg^{-1}), French Polynesia (279.4 g kg^{-1}), and Fiji (268.9 g kg^{-1}) in Oceania. In contrast, the lowest values for clay content occur in Finland (Europe), with a mean value of only 80.5 g kg^{-1}. The mean BD of the soils (Figure 5C) reveals high density in Saudi Arabia and Iran (approximately 1.6 gcm^{-3}) and low density in Russia (1.1 gcm^{-3}). We illustrate the soil-property contents in these countries, which determine soil

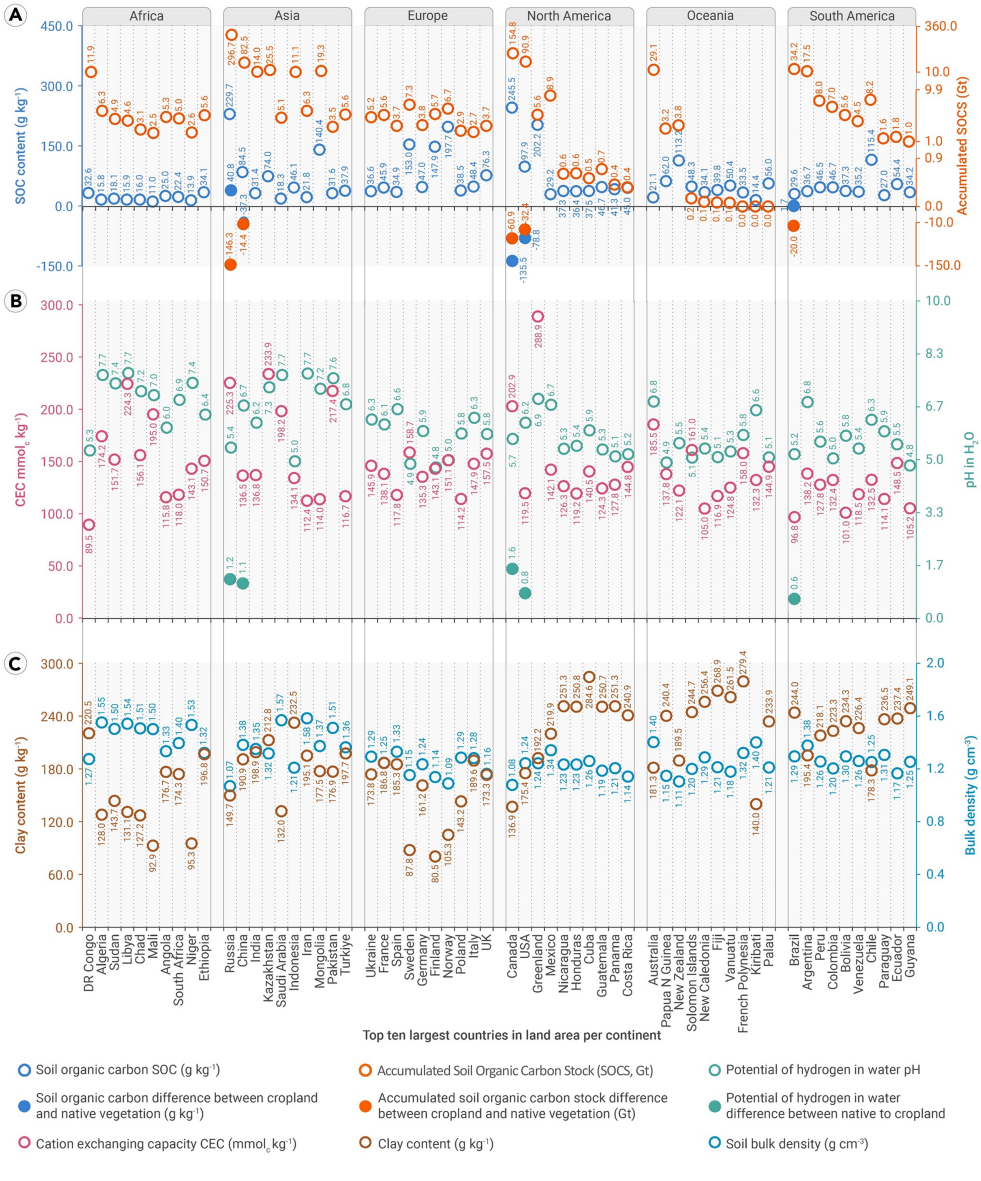

Figure 5. Soil properties chart of the top 10 largest countries in land area per continent (A) Soil organic carbon (SOC) content (blue circles) and soil organic carbon stock (SOCS, orange circles), (B) cation exchange capacity (CEC, pink circles) and pH in water (green circles), and (C) clay content (brown circles) and BD (cyan circles). The respective blue, orange, and green spheres represent the SOC, SOCS, and pH differences between the cultivated areas and the native vegetation.

health and fertility that subsequently drive particular agricultural and forest management.

Distribution of soil properties by socio-economic factors

Among human-induced factors, socio-economic aspects have been understudied concerning soils on a global scale.[82] This overview reveals how countries utilize their resources to maximize their economic capacity and productivity. In addition, identifying soil properties that constrain capacity and productivity provides insights into where targeted management activities (i.e., soil amendments or carbon-smart management practices) impact the sustainable use of resources.

The gross domestic product (GDP) is crucial for assessing the economic size and health of a country and allows the monitoring of economic trends over time.[49] We present relationships between SOCS and pH by GDP as well as SOC and CEC by GDP *per capita* for the top 20 richest, middle-income, and poorest countries, illustrating a second-order polynomial trendline with equations R^2 and RMSE of the model for total and *per capita* GDP (Figures 6A and 6B). SOCSs, for instance, presented 0.56 of R^2 and low RMSE (US$1.13 billion). Although there is no direct correlation between soil pH and countries' GDP (R^2 = 0.05), areas in the Northern Hemisphere show less acidic soils than in the Southern. This may be explained by the predominant alkaline minerals in soils and the drier climate, constraining the water balance in this region. Water balance creates a threshold in soil pH that regulates the soil's capacity for nutrient supply and crop productivity at the global scale.[53] There was an abrupt transition from alkaline to acid soil pH when mean annual precipitation exceeded mean annual potential evapotranspiration in a global dataset of 60,291 pH measurements.

The concept of resource quality is linked to the dynamic human settlement of the Earth, where more prosperous nations have often developed under more favorable conditions, including optimal climate conditions and soil properties critical to soil fertility, quality, health, and, thus, crop productivity. For instance, American societies emerged along rivers and water resources over time (1790–2010), suggesting that favorable water resources support the prosperity of human societies.[83] In analogy to the historical coevolution of water-human systems, our study suggests that societal growth expressed through mapping spatially explicit relations between soil properties and economic success (GDP) is interlinked. In essence, this soil-human nexus provides a direct, geographically primed link between soil health and human prosperity and growth. As a consequence, regions with limited resources could benefit from soil management and tillage practices that can alter soil conditions. Especially, climate-smart management practices, such as no-tillage, reduced tillage, biochar applications, and cover crops,[10] hold promise to enhance SOC, and optimize pH and CEC, boosting crop productivity and economic growth.

Secondly, we observe an exponential trend between a country's economic strength and the level of SOCS (Figure 6A). This trend supports the hypothesis that the oldest communities have historically settled in regions with milder, cooler, and temperate climates, where SOC has accumulated in the soil over longer periods, increasing its fertility. In contrast, the world's poorest regions are generally found in tropical areas where soil organic matter degrades rapidly.[46] Many of the wealthiest nations, corresponding to the highest SOCS values, are also among the largest countries in terms of surface area. As SOCS calculations are based on surface layers, larger countries naturally have an advantage in carbon storage compared to their smaller counterparts. The classification of countries by GDP *per capita* was necessary to constrain the influence of country size (Figure 6B). Higher-income nations had higher SOC and CEC than the poorest ones. For example, the USA, with 90.8-Gt SOCS, had a mean SOC of 97.9 g kg^{-1}. This country was the wealthiest in the total GDP and placed eighth considering the GDP *per capita*. The R^2 for SOC and CEC achieved 0.26 and 0.11, with higher RMSE, demonstrating low potential to predict these socio-economic variables.

Brazil, with a *per capita* income of US$9,550, was in the middle of the ranking with a mean SOC of only 29.6 g kg^{-1} and the highest SOCS (34.2 Gt). Although Mali is the eighth-largest country in Africa, it is classified as a low-income country. Sahara Desert covers a large part of its territory, resulting in very low SOC and SOCS values (11 g kg^{-1} and 2.5 Gt, respectively).

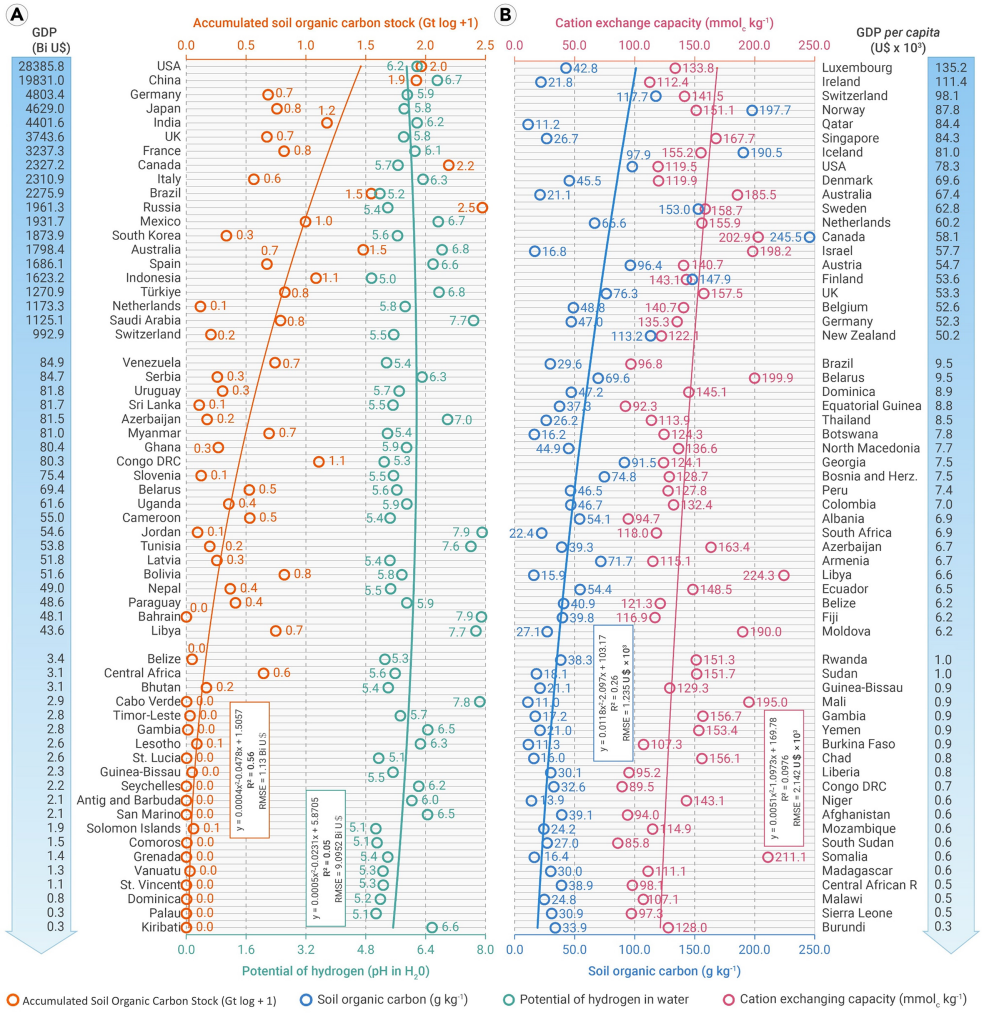

Figure 6. Relationship between soil properties and the top 20 richest, intermediate, and poorest countries (A) Decreasing order according to the gross domestic product (GDP) in billions of dollars, and (B) decreasing order by GDP *per capita* in thousands of dollars. The data considered the mean of the International Monetary Fund's[49] projections for GDP from 2021 to 2028. Soil organic carbon stock (SOCS, orange circles), pH in water (green circles), soil organic carbon (SOC) content (blue circles), and cation exchange capacity (CEC, pink circles). Gt, gigatons; USA, United States of America; UK, United Kingdom; Herz., Bosnia and Herzegovina; DRC, Democratic Republic of Congo; R^2, coefficient of determination; RMSE, root-mean-square error.

SOC mapping using an enhanced dataset of soil and environmental covariates to inspire discussion within the global mapping community. Our soil maps (Figures 1A–1F) focus on profoundly important properties to achieve soil health,[18,52,87] soil mapping,[9] soil productivity,[25] and circular economy in soil.[88] Besides, high-resolution soil spatial information may contribute to agriculture, such as fertilization, the carbon credit market, and precision agriculture.[89,90]

We adopted a transdisciplinary approach that integrates soils with socio-economic and environmental domains. These insights are critical for formulating targeted soil management and conservation strategies to achieve Sustainable Development Goals (SDGs).[91] For example, enhancing soil health in tropical regions with strategies to accumulate more SOC in low-fertility and marginal soils could reduce poverty and hunger by improving agricultural yields and livelihoods (No Poverty, SDG1; Zero Hunger, SDG2). Targeting practices that maintain and promote carbon sequestration in soils supports regional climate action, such as low-carbon agriculture (Climate Action, SDG13).

To increase the discussion on this matter, we observed that the richest countries with higher agriculture gross production value (GPV) had greater SOCS and clay, as the share of the population in poverty correlated with SOC and CEC (Figures S8A and S8B, Supplemental Note 1). Results show a tendency but also indicate the complexity of understanding all the variables involved. Earlier, it was already observed that population pressure and soil quality were strongly negatively correlated in Uganda.[84] However, they also found strong evidence concerning the positive correlation between population pressure and agricultural intensification. A complex discussion arises as observations indicate that rural poverty in degrading agricultural land increased in low-income countries and sub-Saharan Africa and South Asia.[85]

The key to avoiding these problems is to relate soil properties to economic, social, and environmental factors. According to the International Food Policy Research Institute (IFPRI),[86] nearly 40%–75% of the world's agricultural land experiences important impacts on productivity due to soil degradation. In conclusion, the spatial variability (Figure 1) and the relation of the soil properties variations with land use (Figure S6, Supplemental Note 1) shed light on this urgent discussion. It is important to note that evaluating the distribution of soil properties concerning GDP, agriculture GPV, and poverty rates are just some approaches. Other socio-economic data, such as human development and health indices, can also be examined to uncover connections between soil and various sectors.

CONCLUSION

A comprehensive analysis of global soil properties reveals new and significant variations in six soil properties due to heterogeneity in climate, parent materials, topography, and other factors.[2] This approach enabled us to understand the connection between soil health, climatic, biotic, and socio-economic factors that inform targeted human management. We present new results on global

Since we invested substantial effort and time (5+ years) in compiling a new global soil dataset, it is expected to advance findings beyond previous global DSM-derived datasets, mainly from public legacy databases. Thus, new insights into global soil patterns are necessary. The inclusion of RS-derived global spatiotemporal Earth observation data as powerful environmental covariates to improve soil property models is an important advancement. This strategy extrapolates the model to account for the unique regional characteristics.

Future works should prioritize space-time mapping approaches to enhance dynamic soil-attribute prediction and generate comprehensive time-series maps. Dynamic tracking of soil changes due to climate variability and land-use change is hampered by scarce or inconsistent soil-sampling data. Coordinated efforts, including private collaborations to enrich global soil datasets with accurate data information, are essential. Soil minerals in the clay fraction, such as goethite and hematite, have a great influence on SOCS dynamics and sequestration potential[92,93] and, thus, should be addressed in future DSM works. Finally, the present paper contributes to addressing global issues of concern outlined by the Intergovernmental Panel on Climate Change (IPCC; https://www.ipcc.ch/srccl/). Our results are poised to provide the foundation for global soil monitoring and can guide the strategic placement of soil observatories in different geographic regions.

Thus, we successfully developed the first high-resolution global soil grids for key soil properties, with a 90-m pixel size, underpinned by a robust and new Earth observation system. This achievement provides a valuable resource for researchers and policymakers, offering improved spatial detail information. Furthermore, by integrating these soil properties with socio-environmental perspectives, we have gone beyond traditional soil-mapping studies and laid the foundation for more informed, context-sensitive decision-making in land

management, environmental conservation, and sustainable development. Integrating multi-temporal satellite proxies, such as bare soil and vegetation, is a crucial technique for achieving fine-scale, global coverage without gaps in ground data. This method effectively modeled key soil properties with excellent predictive performance, taking into account the vast and diverse soil-environmental conditions around the world.

The findings demonstrated that 64% of the world's topsoils are predominantly sandy, with restricted fertility and susceptible to degradation-limiting crop productivity and highlighting potential risks to food security. We identified that the mean SOC content in cultivated soils is at least 60% lower than under natural vegetation. Global soil pH values were 5.5 in native vegetation and 6.6 in croplands, reflecting the application of fertility soil-management practices. We also revealed that the top 10 largest countries per continent in terms of land area collectively store 75% of the global SOCS, emphasizing that such soil wealth represents a form of land capital closely linked to national economic strength. Overall, we underscore the need to integrate soil and socio-economic factors to bolster carbon marketing, conservation, and climate-smart practices to improve soil health and to discuss sustainability, resilience, and food and human security. This approach represents a significant, challenging step forward in these fields and also paves the way for a deeper understanding of the complex interactions between soil systems and socio-environmental factors.

RESOURCE AVAILABILITY

Material availability

This study did not generate new unique material/reagents.

Data and code availability

The maps generated in this study are publicly available and can be accessed online at https://esalqgeocis.wixsite.com/english/jose-a-m-dematte-global-soil-properties-90m. They can also be accessed and downloaded via the Earth Engine API at https://ee-geocis.projects.earthengine.app/view/global-soil-properties. Any code used in this study is available from the corresponding author upon reasonable request.

FUNDING AND ACKNOWLEDGMENTS

This research was supported by the São Paulo Research Foundation (FAPESP) under grants 2014-22262-0 and 2021/05129-8 as well as the from the Center for Carbon Research in Tropical Agriculture (CCARBON) at the University of São Paulo, under grant 2021/10573-4. We also must mention the support of the MII Project of the Russian Federation (reg. 123030300031-6). The first author acknowledges CNPq for research scholarship (307190-2021-8). We extend our gratitude to international researchers and institutions for contributing soil data, especially the US Department of Agriculture Natural Resources Conservation Service for their coordination, collection, and provision of soil sample data in the USA. We thank the GeoCiS research group (https://esalqgeocis.wixsite.com/english) for their technical support.

AUTHOR CONTRIBUTIONS

Conceptualization, J.A.M.D. and R.R.P.; Formal analysis, R.R.P., J.J.M.N., and N.A.R.; Methodology, R.R.P. and J.J.M.N.; Software, R.R.P. and J.J.M.N.; Visualization, R.R.P., J. J.M.N., M.T.A.A., and N.A.R.; Data curation, J.A.M.D., R.R.P., J.J.M.N., and N.A.R.; Roles/Writing - original draft, J.A.M.D., J.J.M.N., and N.A.R.; Writing - review & editing, J.A.M.D., R.R.P., J.J.M.N., N.A.R., B.M., I.Y.S., S.G., S.C., Y.H., J.H., S.C.C., Q.d.J.v.L., E.B., C.G., Z.G., M.T.A.A., L. G.V., J.T.F.R., R.M., A.G., A.V.Z., J.P.C., Y.M., H.J.J., R., C.W., R.R., N.T., N.Ts., M.K., D.N.K., S.D., Y.G., E.V., S.A., J.K.M.B., A.B., S.N.M., N.A.H., E.K., D.C.M., M.R.F., E.S.M.S., and A.A.; Validation, J.A.M.D., R.R.P., N.A.R., J.J.M.N.; Funding acquisition, Resources, Supervision, J.A.M.D. All authors contributed to the manuscript and approved the final version.

DECLARATION OF INTERESTS

The authors declare no conflict of interest.

SUPPLEMENTAL INFORMATION

It can be found online at https://doi.org/10.1016/j.xinn.2025.100985.

REFERENCES

1. Bardgett, R.D. and van der Putten, W.H. (2014). Belowground biodiversity and ecosystem functioning. *Nature* **515**:505–511. DOI:https://doi.org/10.1038/nature13855.
2. Lal, R., Bouma, J., Brevik, E. et al. (2021). Soils and sustainable development goals of the United Nations: An International Union of Soil Sciences perspective. *Geoderma Reg.* **25**: e00398. DOI:https://doi.org/10.1016/j.geodrs.2021.e00398.
3. Eekhout, J.P.C. and de Vente, J. (2022). Global impact of climate change on soil erosion and potential for adaptation through soil conservation. *Earth Sci. Rev.* **226**:103921. DOI: https://doi.org/10.1016/j.earscirev.2022.103921.
4. Guerra, C.A., Berdugo, M., Eldridge, D.J. et al. (2022). Global hotspots for soil nature conservation. *Nature* **610**:693–698. DOI:https://doi.org/10.1038/s41586-022-05292-x.
5. Friedlingstein, P., O'Sullivan, M., Jones, M.W. et al. (2023). Global Carbon Budget 2023. *Earth Syst. Sci. Data* **15**:5301–5369. DOI:https://doi.org/10.5194/essd-15-5301-2023.
6. Georgiou, K., Jackson, R.B., Vindušková, O. et al. (2022). Global stocks and capacity of mineral-associated soil organic carbon. *Nat. Commun.* **13**:3797. DOI:https://doi.org/10.1038/s41467-022-31540-9.
7. Scharlemann, J.P., Tanner, E.V., Hiederer, R. et al. (2014). Global soil carbon: Understanding and managing the largest terrestrial carbon pool. *Carbon Manag.* **5**:81–91. DOI:https://doi.org/10.4155/cmt.13.77.
8. Wang, F., Harindintwali, J.D., Wei, K. et al. (2023). Climate change: Strategies for mitigation and adaptation. *Innov. Geosci.* **1**:100015. DOI:https://doi.org/10.59717/j.xinn-geo.2023.100015.
9. McBratney, A., Field, D.J. and Koch, A. (2014). The dimensions of soil security. *Geoderma* **213**:203–213. DOI:https://doi.org/10.1016/j.geoderma.2013.08.013.
10. Paustian, K., Lehmann, J., Ogle, S. et al. (2016). Climate-smart soils. *Nature* **532**:49–57. DOI:https://doi.org/10.1038/nature17174.
11. Vereecken, H., Amelung, W., Bauke, S.L. et al. (2022). Soil hydrology in the Earth system. *Nat. Rev. Earth Environ.* **3**:573–587. DOI:https://doi.org/10.1038/s43017-022-00324-6.
12. Boretti, A. and Rosa, L. (2019). Reassessing the projections of the World Water Development Report. *npj Clean Water* **2**:15. DOI:https://doi.org/10.1038/s41545-019-0039-9.
13. Grunwald, S. (2022). Artificial intelligence and soil carbon modeling demystified: Power, potentials, and perils. *Carbon Footprints* **1**:6. DOI:https://doi.org/10.20517/cf.2022.03.
14. Padarian, J., Stockmann, U., Minasny, B. et al. (2022). Monitoring changes in global soil organic carbon stocks from space. *Remote Sens. Environ.* **281**:113260. DOI:https://doi.org/10.1016/j.rse.2022.113260.
15. Padarian, J., Minasny, B., McBratney, A. et al. (2022). Soil carbon sequestration potential in global Croplands. *PeerJ* **10**:e13740. DOI:https://doi.org/10.7717/peerj.13740.
16. Lembrechts, J.J., van den Hoogen, J., Aalto, J. et al. (2022). Global maps of soil temperature. *Glob. Change Biol.* **28**:3110–3144. DOI:https://doi.org/10.1111/gcb.16060.
17. Lenton, T.M., Xu, C., Abrams, J.F. et al. (2023). Quantifying the human cost of global warming. *Nat. Sustain.* **6**:1237–1247. DOI:https://doi.org/10.1038/s41893-023-01132-6.
18. Poppiel, R.R., Cherubin, M.R., Novais, J.J.M. et al. (2025). Soil health in Latin America and the Caribbean. *Commun. Earth Environ.* **6**:141. DOI:https://doi.org/10.1038/s43247-025-02021-w.
19. Batjes, N.H. (2016). Harmonized soil property values for broad-scale modeling (WISE30sec) with estimates of global soil carbon stocks. *Geoderma* **269**:61–68. DOI: https://doi.org/10.1016/j.geoderma.2016.01.034.
20. Poggio, L., de Sousa, L.M., Batjes, N.H. et al. (2021). SoilGrids 2.0: producing soil information for the globe with quantified spatial uncertainty. *Soil* **7**:217–240. DOI:https://doi.org/10.5194/soil-7-217-2021.
21. Lotfollahi, L., Delavar, M.A., Biswas, A. et al. (2023). Modeling the Spatial Distribution of Sand, Silt, and Clay Particles Based on Global Soil Map and Limited Data. *J. Desert Res.* **23**:123–137. DOI:https://doi.org/10.22059/jdesert.2023.95533.
22. Xiang, D., Wang, G., Tian, J. et al. (2023). Global patterns and edaphic-climatic controls of soil carbon decomposition kinetics predicted from incubation experiments. *Nat. Commun.* **14**:2171. DOI:https://doi.org/10.1038/s41467-023-37900-3.
23. Lin, Z., Dai, Y., Mishra, U. et al. (2024). Global and regional soil organic carbon estimates: Magnitude and uncertainties. *Pedosphere* **34**:685–698. DOI:https://doi.org/10.1016/j.pedsph.2023.06.005.
24. Dynarski, K.A., Bossio, D.A. and Scow, K.M. (2020). Dynamic stability of soil carbon: Reassessing the "permanence" of soil carbon sequestration. *Front. Environ. Sci.* **8**:1–14. DOI:https://doi.org/10.3389/fenvs.2020.514701.
25. Greschuk, L.T., Demattê, J.A.M., Silvero, N.E.Q. et al. (2023). A soil productivity system reveals most Brazilian agricultural lands are below their maximum potential. *Sci. Rep.* **13**:14103. DOI:https://doi.org/10.1038/s41598-023-39981-y.
26. Evangelista, S.J., Field, D.J., McBratney, A.B. et al. (2023). A proposal for the assessment of soil security: Soil functions, soil services and threats to soil. *Soil Secur.* **10**:100086. DOI: https://doi.org/10.1016/j.soisec.2023.100086.
27. Peng, Y., Ben-Dor, E., Biswas, A. et al. (2025). Spectroscopic solutions for generating new global soil information. *Innovation* **6**:100839. DOI:https://doi.org/10.1016/j.xinn.2025.100839.
28. Rogge, D., Bauer, A., Zeidler, J. et al. (2018). Building an exposed soil composite processor (SCMaP) for mapping spatial and temporal characteristics of soils with Landsat imagery (1984–2014). *Remote Sens. Environ.* **205**:1–17. DOI:https://doi.org/10.1016/j.rse.2017.11.004.
29. Demattê, J.A.M., Fongaro, C.T., Rizzo, R. et al. (2018). Geospatial Soil Sensing System (GEOS3): A powerful data mining procedure to retrieve soil spectral reflectance from satellite images. *Remote Sens. Environ.* **212**:161–175. DOI:https://doi.org/10.1016/j.rse.2018.04.047.
30. Xue, J., Zhang, X., Huang, Y. et al. (2024). A two-dimensional bare soil separation framework using multi-temporal Sentinel-2 images across China. *Int. J. Appl. Earth Obs. Geoinf.* **134**:104181. DOI:https://doi.org/10.1016/j.jag.2024.104181.

31. Durán, J. and Delgado-Baquerizo, M. (2020). Vegetation structure determines the spatial variability of soil biodiversity across biomes. *Sci. Rep.* **10**:21500. DOI:https://doi.org/10.1038/s41598-020-78483-z.
32. Arrouays, D., Poggio, L., Salazar Guerrero, O.A. et al. (2020). Digital soil mapping and GlobalSoilMap: Main advances and ways forward. *Geoderma Reg.* **21**:e00265. DOI:https://doi.org/10.1016/j.geodrs.2020.e00265.
33. Barman, K.G., Caron, S., Claassen, T. et al. (2024). Towards a benchmark for scientific understanding in humans and machines. *Minds Mach.* **34**:6. DOI:https://doi.org/10.1007/s11023-024-09657-1.
34. Bishop, T.F.A., McBratney, A.B. and Laslett, G.M. (1999). Modelling soil attribute depth functions with equal-area quadratic smoothing splines. *Geoderma* **91**:27–45. DOI:https://doi.org/10.1016/S0016-7061(99)00003-8.
35. Chen, S., Dai, L., Shuai, Q. et al. (2022). Global Soil Bulk Density DataBase (GSBDDB) (V1.0). *Zenodo*. DOI:https://doi.org/10.5281/zenodo.7075158.
36. McBratney, A.B., Mendonça Santos, M.L. and Minasny, B. (2003). On digital soil mapping. *Geoderma* **117**:3–52. DOI:https://doi.org/10.1016/S0016-7061(03)00223-4.
37. Gorelick, N., Hancher, M., Dixon, M. et al. (2017). Google Earth Engine: Planetary-scale geospatial analysis for everyone. *Remote Sens. Environ.* **202**:18–27. DOI:https://doi.org/10.1016/j.rse.2017.06.031.
38. Demattê, J.A.M., Rizzo, R., Rosin, N.A. et al. (2025). A global soil spectral grid based on space sensing. *Sci. Total Environ.* **968**:178791. DOI:https://doi.org/10.1016/j.scitotenv.2025.178791.
39. Karger, D.N., Conrad, O., Böhner, J. et al. (2017). Climatologies at high resolution for the Earth land surface areas. *Sci. Data* **4**:170122. DOI:https://doi.org/10.1038/sdata.2017.122.
40. Safanelli, J., Poppiel, R., Ruiz, L. et al. (2020). Terrain analysis in Google Earth Engine: A method adapted for high-performance global-scale analysis. *ISPRS Int. J. GeoInf.* **9**:400. DOI:https://doi.org/10.3390/ijgi9060400.
41. Theobald, D.M., Harrison-Atlas, D., Monahan, W.B. et al. (2015). Ecologically-relevant maps of landforms and physiographic diversity for climate adaptation planning. *PLoS One* **10**:e0143619. DOI:https://doi.org/10.1371/journal.pone.0143619.
42. Yamazaki, D., Ikeshima, D., Tawatari, R. et al. (2017). A high accuracy map of global terrain elevations. *Geophys. Res. Lett.* **44**:5844–5853. DOI:https://doi.org/10.1002/2017GL072874.
43. Behrens, T., Schmidt, K., Viscarra Rossel, R.A. et al. (2018). Spatial modelling with Euclidean distance fields and machine learning. *Eur. J. Soil Sci.* **69**:757–770. DOI:https://doi.org/10.1111/ejss.12687.
44. van den Hoogen, J., Gerten, D., van Bodegom, P.M. et al. (2021). A geospatial mapping pipeline for ecologists. Preprint at *bioRxiv*. https://www.researchgate.net/publication/353150945_A_geospatial_mapping_pipeline_for_ecologists.
45. Breiman, L. (2001). Random Forests. *Mach. Learn.* **45**:5–32. DOI:https://doi.org/10.1023/A:1010933404324.
46. Beck, H.E., McVicar, T.R., Vergopolan, N. et al. (2023). High-resolution (1 km) Köppen-Geiger maps for 1901–2099 based on constrained CMIP6 projections. *Sci. Data* **10**:724. DOI:https://doi.org/10.1038/s41597-023-02549-6.
47. Olson, D.M., Dinerstein, E., Wikramanayake, E.D. et al. (2001). Terrestrial ecoregions of the world: A new map of life on Earth. *Bioscience* **51**:933. DOI:https://doi.org/10.4236/oje.2022.123014.
48. Zanaga, D., Van De Kerchove, R., Daems, D. et al. (2022). ESA WorldCover 10 m 2021 v200. *Zenodo*. DOI:https://doi.org/10.5281/zenodo.7254220.
49. International Monetary Fund – IMF (2023). World Economic Outlook Database, October 2023. https://www.imf.org/en/Publications/WEO/weo-database/2023/October.
50. Food and Agriculture Organization of the United Nations (2024). Gross production value of the agricultural sector. Our World in Data (with major processing). https://ourworldindata.org/grapher/value-of-agricultural-production.
51. World Bank (2024). Share of population living in extreme poverty. Our World in Data (with major processing). https://ourworldindata.org/poverty.
52. Lehmann, J., Bossio, D.A., Kögel-Knabner, I. et al. (2020). The concept and future prospects of soil health. *Nat. Rev. Earth Environ.* **1**:544–553. DOI:https://doi.org/10.1038/s43017-020-0080-8.
53. Slessarev, E.W., Lin, Y., Bingham, N.L. et al. (2016). Water balance creates a threshold in soil pH at the global scale. *Nature* **540**:567–569. https://www.nature.com/articles/nature20139.
54. Brus, D.J. (2019). Sampling for digital soil mapping: A tutorial supported by R scripts. *Geoderma* **338**:464–480. DOI:https://doi.org/10.1016/j.geoderma.2018.07.036.
55. Somarathna, P.D.S.N., Minasny, B. and Malone, B.P. (2017). More data or a better model? Figuring out what matters most for the spatial prediction of soil carbon. *Soil Sci. Soc. Am. J.* **81**:1413–1426. DOI:https://doi.org/10.2136/sssaj2016.11.0376.
56. Hengl, T., de Jesus, J.M., MacMillan, R.A. et al. (2014). SoilGrids1km — Global Soil Information Based on Automated Mapping. *PLoS One* **9**:e105992. DOI:https://doi.org/10.1371/journal.pone.0105992.
57. van Wesemael, B., Abdelbaki, A., Ben-Dor, E. et al. (2024). A European soil organic carbon monitoring system leveraging Sentinel 2 imagery and the LUCAS soil database. *Geoderma* **452**:117113. DOI:https://doi.org/10.1016/j.geoderma.2024.117113.
58. Hiederer, R. and Köchy, M. (2011). Global Soil Organic Carbon Estimates and the Harmonized World Soil Database (Publ. Off. Eur. Union). DOI:https://doi.org/10.2788/13267.
59. Batjes, N.H., Ribeiro, E. and van Oostrum, A. (2020). Standardised soil profile data to support global mapping and modelling (WoSIS snapshot 2019). *Earth Syst. Sci. Data* **12**:299–320. DOI:https://doi.org/10.5194/essd-12-299-2020.
60. United Nations (2018). Global Soil Organic Carbon Map (GSOCmap). *FAO Tech. Rep.* **1**:162. https://www.fao.org/3/I8891EN/i8891en.pdf.
61. Piedallu, C., Pedersoli, E., Chaste, E. et al. (2022). Optimal resolution of soil properties maps varies according to their geographical extent and location. *Geoderma* **412**:115723. DOI:https://doi.org/10.1016/j.geoderma.2022.115723.
62. Garosi, Y., Ayoubi, S., Nussbaum, M. et al. (2022). Effects of different sources and spatial resolutions of environmental covariates on prediction of soil organic carbon using machine learning in a semi-arid region of Iran. *Geoderma Reg.* **29**:e00513. DOI:https://doi.org/10.1016/j.geodrs.2022.e00513.
63. Guo, L., Shi, T., Linderman, M. et al. (2019). Exploring the influence of spatial resolution on the digital mapping of soil organic carbon by airborne hyperspectral VNIR Imaging. *Remote Sens.* **11**:1032. DOI:https://doi.org/10.3390/rs11091032.
64. Zhang, S., Zhu, Q., de Vries, W. et al. (2023). Effects of soil amendments on soil acidity and crop yields in acidic soils: A world-wide meta-analysis. *J. Environ. Manage.* **345**:118531. DOI:https://doi.org/10.1016/j.jenvman.2023.118531.
65. Raza, S., Zamanian, K., Ullah, S. et al. (2021). Inorganic carbon losses by soil acidification jeopardize global efforts on carbon sequestration and climate change mitigation. *J. Clean. Prod.* **315**:128036. DOI:https://doi.org/10.1016/j.jclepro.2021.128036.
66. Berthrong, S.T., Jobbágy, E.G. and Jackson, R.B. (2009). A global meta-analysis of soil exchangeable cations, pH, carbon, and nitrogen with afforestation. *Ecol. Appl.* **19**:2228–2241. DOI:https://doi.org/10.1890/08-1730.1.
67. Xu, L., He, N. and Yu, G. (2016). Methods of evaluating soil bulk density: Impact on estimating large scale soil organic carbon storage. *Catena* **144**:94–101. DOI:https://doi.org/10.1016/j.catena.2016.05.001.
68. AL-Shammary, A.A.G., Kouzani, A.Z., Kaynak, A. et al. (2018). Soil Bulk Density Estimation Methods: A Review. *Pedosphere* **28**:581–596. DOI:https://doi.org/10.1016/S1002-0160(18)60034-7.
69. Khaledian, Y., Brevik, E.C., Pereira, P. et al. (2017). Modeling soil cation exchange capacity in multiple countries. *Catena* **158**:194–200. DOI:https://doi.org/10.1016/j.catena.2017.07.002.
70. Stockmann, U., Padarian, J., McBratney, A. et al. (2015). Global soil organic carbon assessment. *Global Food Secur.* **6**:9–16. DOI:https://doi.org/10.1016/j.gfs.2015.07.001.
71. Neina, D. (2019). The role of soil pH in plant nutrition and soil remediation. *Appl. Environ. Soil Sci.* **2019**:1–9. DOI:https://doi.org/10.1155/2019/5794869.
72. Zhao, X., Yang, Y., Shen, H. et al. (2019). Global soil–climate–biome diagram: linking surface soil properties to climate and biota. *Biogeosciences* **16**:2857–2871. DOI:https://doi.org/10.5194/bg-16-2857-2019.
73. Powell, T.L., Davis, T.S. and Cousins, A.B. (2021). Global influence of soil texture on ecosystem water limitation. *Nature* **593**:549–552. DOI:https://doi.org/10.1038/s41586-024-08089-2.
74. Turek, M.E., Poggio, L., Batjes, N.H. et al. (2023). Global mapping of volumetric water retention at 100, 330, and 15 000 cm suction using the WoSIS database. *Int. Soil Water Conserv. Res.* **11**:225–239. DOI:https://doi.org/10.1016/j.iswcr.2022.08.001.
75. Sanderman, J., Hengl, T. and Fiske, G.J. (2017). Soil carbon debt of 12,000 years of human land use. *Proc. Natl. Acad. Sci. USA* **114**:9575–9580. DOI:https://doi.org/10.1073/pnas.1706103114.
76. Bansal, S., Creed, I.F., Tangen, B.A. et al. (2023). Practical guide to measuring wetland carbon pools and fluxes. *Wetlands* **43**:105. DOI:https://doi.org/10.1007/s13157-023-01722-2.
77. de Freitas, I.C., Ribeiro, J.M., Araújo, N.C.A. et al. (2020). Agrosilvopastoral systems and well-managed pastures increase soil carbon stocks in the Brazilian Cerrado. *Rangel. Ecol. Manag.* **73**:776–785. DOI:https://doi.org/10.1016/j.rama.2020.08.001.
78. Koudahe, K., Allen, S.C. and Djaman, K. (2022). Critical review of the impact of cover crops on soil properties. *Int. Soil Water Conserv. Res.* **10**:343–354. DOI:https://doi.org/10.1016/j.iswcr.2022.03.003.
79. Bowles, T.M., Mooshammer, M., Socolar, Y. et al. (2020). Long-term evidence shows that crop rotation diversification increases agricultural resilience to adverse growing conditions in North America. *One Earth* **2**:284–293. DOI:https://doi.org/10.1016/j.oneear.2020.02.007.
80. Daryanto, S., Fu, B., Wang, L. et al. (2018). Quantitative synthesis on the ecosystem services of cover crops. *Earth Sci. Rev.* **185**:357–373. DOI:https://doi.org/10.1016/j.earscirev.2018.06.013.
81. Noulas, C., Tziouvalekas, M. and Karyotis, T. (2018). Zinc in soils, water and food crops. *J. Trace Elem. Med. Biol.* **49**:252–260. DOI:https://doi.org/10.1016/j.jtemb.2018.02.009.
82. Grunwald, S. (2021). Grand challenges in pedometrics-AI research. *Front. Soil Sci.* **1**:1–8. DOI:https://doi.org/10.3389/fsoil.2021.714323.
83. Fang, Y. and Jawitz, J.W. (2019). The evolution of human population distance to water in the USA from 1790 to 2010. *Nat. Commun.* **10**:430. DOI:https://doi.org/10.1038/s41467-019-08366-z.
84. Mugizi, F.M.P. and Matsumoto, T. (2021). A curse or a blessing? Population pressure and soil quality in Sub-Saharan Africa: Evidence from rural Uganda. *Ecol. Econ.* **179**:106851. DOI:https://doi.org/10.1016/j.ecolecon.2020.106851.
85. Barbier, E.B. and Hochard, J.P. (2018). Land degradation and poverty. *Nat. Sustain.* **1**:623–631. DOI:https://doi.org/10.1038/s41893-018-0155-4.
86. Food and Agriculture Organization of the United Nations (2023). The State of Food and Agriculture 2023: Revealing the True Cost of Food to Transform Agrifood Systems, **1** (Rome: FAO), p. 150. https://doi.org/10.4060/cc7724en.
87. Novais, J.J.M., Melo, B.M.D., Neves Junior, A.F. et al. (2025). Online analysis of Amazon's soils through reflectance spectroscopy and cloud computing can support policies and the sustainable development. *J. Environ. Manage.* **375**:124155. DOI:https://doi.org/10.1016/j.jenvman.2025.124155.

88. Nwaogu, C., Minasny, B., Field, D.J. et al. (2025). Conceptualizing core aspects of circular economy in soil: A critical review and analysis. *Crit. Rev. Environ. Sci. Technol.* **55**:805–835. DOI:https://doi.org/10.1080/10643389.2025.2454689.
89. Lawrence, P.G., Roper, W., Morris, T.F. et al. (2020). Guiding soil sampling strategies using classical and spatial statistics: A review. *Agron. J.* **112**:493–510. DOI:https://doi.org/10.1002/agj2.20048.
90. Padhiary, M., Saha, D., Kumar, R. et al. (2024). Enhancing precision agriculture: A comprehensive review of machine learning and AI vision applications in all-terrain vehicle for farm automation. *Smart Agric. Technol.* **8**:100483. DOI:https://doi.org/10.1016/j.atech.2024.100483.
91. United Nations. Transforming Our World (2015). The 2030 Agenda for Sustainable Development, **1** (New York: United Nations), p. 41. https://sdgs.un.org/publications/transforming-our-world-2030-agenda-sustainable-development-17981.
92. Wieder, W.R., Bonan, G.B. and Allison, S.D. (2013). Global soil carbon projections are improved by modelling microbial processes. *Nat. Clim. Change* **3**:909–912. DOI:https://doi.org/10.1038/nclimate1951.
93. Rodríguez-Albarracín, H.S., Demattê, J.A.M., Rosin, N.A. et al. (2024). Soil organic carbon sequestration potential explained by mineralogical and microbiological activity using spectral transfer functions. *Sci. Total Environ.* **947**:174652. DOI:https://doi.org/10.1016/j.scitotenv.2024.174652.